THERMAL ENVIRONMENT PREDICTION USING CFD WITH A VIRTUAL MANNEQUIN MODEL AND EXPERIMENT WITH SUBJECT IN A FLOOR HEATING ROOM

Ryoichi Kajiya[1], Kodai Hiruta[2], Koji Sakai[1], Hiroki Ono[1], Toshihiko Sudo[3]
[1]School of Science and Technology, Meiji University, Japan
[2]AXS Satow Inc., Japan
[3]Nikken Sekkei Research Institute, Japan

ABSTRACT

For the surface temperature of clothing, body surface temperature, and detailed temperatures and heat flow phenomena of soles contacting the floor, results of measurement experiments using human subjects were compared with results of simulations conducted by CFD using a thermal mannequin.
The surface temperature of clothes, body surface temperature, and conduction heat quantity at soles contacting the floor of the numerical thermal mannequin generally agreed with results of actual measurements. Consequently, it was confirmed that warmer environments considering human body in the floor heated room can be reproduced generally by CFD analysis using a thermal mannequin considering contact thermal conduction.

INTRODUCTION

In Japan, because of the remarkable development of science and technology and because of improved living standards, heating facilities have become indispensable. However, of all energy consumption of residences in high-latitude regions, more than one-third is used for heating. Therefore, effective utilization of heating energy is the most important matter for energy saving. The simultaneous pursuit of amenity and energy saving features is therefore strongly demanded for planning of next-generation air-conditioning equipment. To assess the thermal amenity of the human body appropriately, quantitative and stepwise elucidation of heat transfer of three types—radiation, convection, and conduction—is extremely important. However, few conventional studies have addressed these matters comprehensively (Tanabe et al., 1994, Ogasawara1 et al., 2009, Omori et al., 2009,2007). Therefore, this study is aimed at establishment of an assessment method for thermal amenity performance at heating. To investigate the efficacy of CFD in grasping thermal conduction phenomena of the human body and warmer environments around the human body, CFD analysis using a numerical thermal mannequin, considering contact thermal conduction, was conducted along with measurement experiments using human subjects.
The authors performed CFD analysis using a quantitative thermal mannequin in the floor heated room and confirmed the general reproducibility of actual measurements of human subjects (Kajiya et al., 2010,2009). However, because this quantitatively accurate thermal mannequin does not contact with the floor, such a problem arose that contact and the consequent thermal conduction of soles was not reproduced. For that reason, for statistical and detailed modeling of the human body heat balance including conduction in addition to convection and radiation, we performed CFD analysis of a floor heated room using a thermal mannequin, particularly considering contact thermal conduction. The surface temperature of clothes, body surface temperature, detailed temperature and heat flow at the soles contacting the floor, and air temperature and wall surface temperature obtained by CFD analysis were compared with results of measurement experiments using human subjects to confirm the usability of CFD analysis for environment prediction of this type.

OUTLINE OF MEASUREMENT EXPERIMENTS

Experiments using human subjects were performed in a model of a floor heating room (width 1.8 m × depth 1.8 m × height 2.1 m) installed in a constant temperature room (room temperature controlled to about 5°C). Figure 1 presents an outline of the model of the floor heating room. An electric-type heating panel was provided on the floor of the model room. The input heat quantity was controlled using a transformer. Table 1 portrays the thermal resistance of each wall surface. The overall heat transfer coefficient outside the room for calculation of heat transfer coefficient was set to 9 W/(m^2 · K). The temperature in the constant temperature room was set to 5°C.
Figure 2 depicts positions of human subjects. Figure 3 presents postures and scenes of the experiment. During the experiment, human subjects were located around the center of the room and sitting in a chair was used for the postures of all participants. Temperature measurement poles (Pole 1 and Pole 2) were placed at two locations in front of and behind the human subjects; a heat flow meter was placed at the feet of human subjects to measure conduction of heat through contact. Table 2 presents a list of experimental cases. The input heat quantity was changed in Case 1–3 in the experiment.

All clothes except for underwear (sweat shirt and sweat pants, short sleeve T-shirt, underwear, socks) were designated. The human subjects remained quiet for 30 min in the preparation room (room temperature, 25°C) before starting the experiment and were exposed to the measurement experiment for 1 hr. For Case 1, 25 human subjects participated, as did 4 people each for Case 2 and Case 3. Figure 4 shows measuring points 16 regions.

Measurements were limited to the left of human subjects; Fig. 5 shows measuring points on their soles. Human bodies were classified into side of the body. To grasp contact thermal conduction in detail, soles were divided into eight regions and measurements were limited to the left foot. Fig. 6 shows measuring points of vertical temperatures; Figure 7 portrays measuring points on the wall surface.

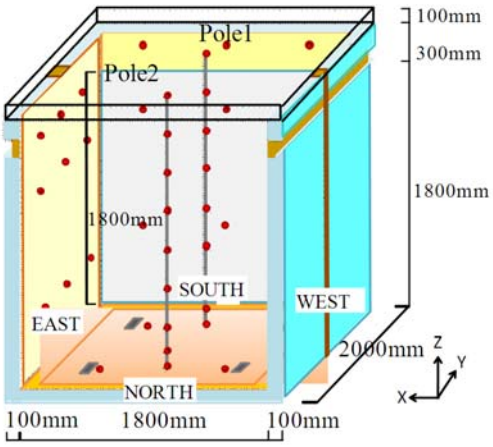

Figure 1 Outline of floor-heated room.

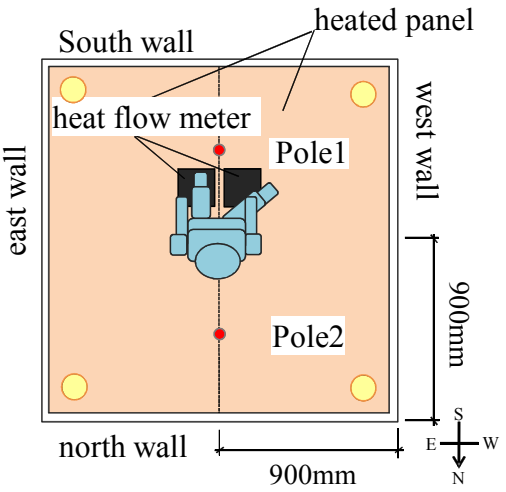

Figure 2 Outline of model room interior.

Table 1 Composition of each wall surface and thermal resistance

parts of room	Constitution materials of the wall	thermal resistance [(m^2·K)/W]
sourth wall	insulation material 100mm + glass 6mm	2.821
other walls	insulation material 100mm + plywood 12mm + veneer 2.3mm	2.909
ceiling	insulation material 100mm + plywood 12mm + veneer 2.3mm	2.822
floor	insulation material 50mm + plywood 12mm ×2	1.621
beam and pillar	wood 90mm + plywood 12mm + veneer 2.3mm	0.849
	wood 76mm + plywood 12mm + veneer 2.3mm	0.749

Figure 3 Postures of human subjects and the scene of the experiment.

Table 2 Measurement case and attributes of human subjects

Case No.		Case1	Case2	Case3
posture of human subjects		chair sitting		
number of subjects	male	15	2	2
	female	10	2	2
input heat quantity[W]		145.2	177.6	116.1
temperature of floor surface [℃]		26	29	23
kind of the clothing		sweat shirt,sweatpants, short sleeve T-shirt, underwear and socks		
temperature of cnstannt temperature room		5[℃]		
standby time		30min.		
measurement time		60min.		

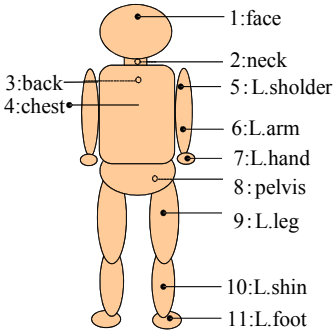

Figure 4 Temperature measurement points on the human body.

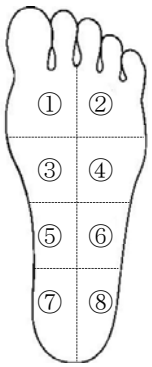

Figure 5 Temperature measurement points at the foot soles.

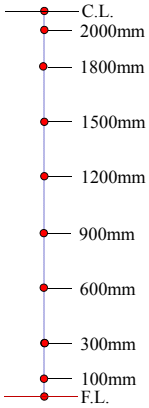

Figure 6 Measuring points of vertical temperatures.

OUTLINE OF CFD ANALYSIS

Analysis subjects participated in measurement experiments. Room interiors and the human body were modeled as close to the actual conditions as possible. Three analytical cases were specified (Case 1, 2, and 3) similarly to the measurement experiment. Commercial code (STAR-CD ver. 4.10; CDA Japan) was used for CFD analysis. A low Reynolds number type k-ε model was used for the turbulence model, the SIMPLE method was used for the calculation algorithm, MARS was used for a difference scheme, radiant flux was 1024, and the area element size was identical to that of the partition unit of the boundary conditions. The discrete beam method was used for radiative analysis: a basic mesh division of 50 mm was used for mesh, the wall surface proximity was fractionized to about 1.6 mm, and the lattice number was set to 273,072 meshes. A solid cell (thermal conductivity, 0.151 W/(m・K); specific heat, 1300 J/(kg・K); density, 856 kg/m^3) equivalent to flooring of target experimental laboratory was used for the floor. The floor heating plane temperature was set to obtain floor surface temperatures of 23°C, 26°C, and 29°C.

Regarding the human body model, a numerical thermal mannequin of an adult male scale and chair sitting posture described by Ito et al.(2006) were used. Figure 8 presents the mesh composition of the human body model used for analysis. The human body model comprises as many as 15,577 individual plane elements, divided into 18 regions. The thermal resistance value obtained by Equation (1) was set as the thermal resistance from the core to clothing surface. Table 3 portrays the thermal resistance of each region. The temperature of the core portion of the human body model was fixed to 36.4°C at all times. Figure 9 presents details of sole contact with the floor.

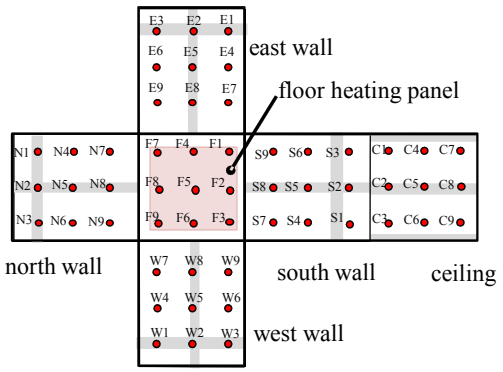

Figure 7 Measuring points of the wall surface temperature (CFD boundary conditions).

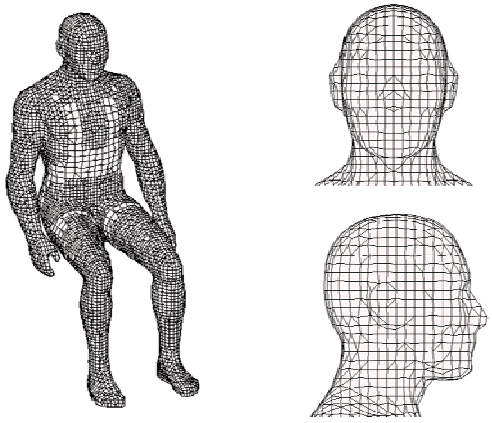

Figure 8 Mesh composition of the human body model.

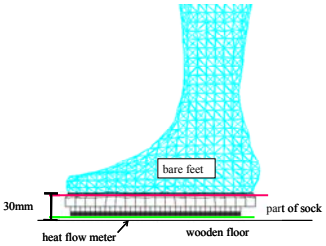

Figure 9 Details of the foot region of the human body model.

DISCUSSION and RESULT ANALYSIS

Figure 10 portrays a vertical temperature profile ofPole 1; Fig. 11 shows the same for Pole 2 as a comparison between experimental and values obtained from analysis. Although the trend of vertical temperature profile of the experimental value and analysis value generally agreed, the analysis value was higher than the experimental value in all cases. This trend became remarkable in Case 1 and Case 3 of Pole 1, although a maximum of about 2°C difference was found in Case 1 and maximum about 1°C difference was found in Case 3. This is be regarded as attributable to differences of human body calorific value because of differences of the body surface area resulting from differences of physical constitution between human subjects and the human model. In Case 1 of Pole 2, the temperature at 0. 9 m above the floor is higher than the temperature at other heights. It is considered that this is influenced by personal differences such as postures and the position of the human subjects: sitting in a chair.

Surface temperature of clothes

Figure 12 portrays a comparison of values obtained from analysis and actual measurements of surface temperatures of clothes in each case. Results show that, for surface temperature of clothes, values obtained from analysis are higher than actual measurements at the shoulder, arm, shin, etc. This is regarded as attributable to the fact that, in actual measurements, an air layer is generated between clothes and body surface. The thermal resistance of clothes became higher than the thermal resistance shown by the analysis. Analysis values of the left foot are higher than actual measurements, although surface temperatures of the clothes at the chest region are nearly identical to the actual measurements. At the feet in Case 3, where the floor surface temperature is low, differences between values obtained from analysis and actual measurements are greater than in other cases. It is about 5°C higher than actual measurements. Apparently, heat dissipation phenomena at the human body extremities are not reproduced exactly by CFD.

Skin surface temperature

Figure 13 portrays a comparison of values obtained from analysis and actual measurement of skin surface temperatures in each case. In Case 1, values obtained from analysis and actual measurements of skin surface temperatures show good agreement. However, in Case 2 and Case 3, temperatures around the core of the body such as the chest and back show generally good agreement, but some differences are apparent at the end part of the human body such as at the hand or foot. Particularly, the difference in Case 3 is remarkable and values obtained from analysis at the foot are

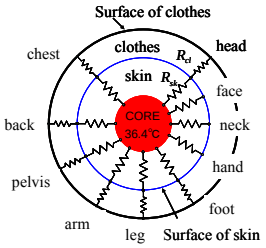

$$R_{sk} = 0.058$$

$$R = R_{sk} + 0.155R_{cl} \quad (1)$$

Where

R : All thermal resistance of the clothing

R_{cl} : Thermal resistance from the core to the skin

R_{sk} : Thermal resistance from the skin to environment

Table 3 Thermal resistance of the human body model

region of body	clo value [clo]	thermal resistance [(m²·K)/W]
head	1.721	0.321
face	(0.033)	0.059
neck	(0.033)	0.059
chest	1.331	0.260
back	1.570	0.297
R-sholder	1.228	0.244
L-sholder	1.204	0.241
R-arm	0.613	0.149
L-arm	0.958	0.203
R-hand	0.079	0.066
L-hand	0.128	0.074
pelvis	1.762	0.327
R-leg	0.576	0.143
L-leg	0.591	0.146
R-shin	0.608	0.148
L-shin	0.626	0.151
R-foot	0.252	0.093
L-foot	0.253	0.093
socks	–	0.047

about 5.5°C higher. Regarding actual measurements, a remarkable decrease in the temperature is apparent at extremities such as feet, but this is not reproduced by the value obtained from analysis. Differences between analysis value of 3D heat dissipation at end part and actual measurements are regarded as a major contributing factor for this. Therefore, setting of boundary conditions of the human body in CFD should be reviewed. The temperature of the distal end of the human body is influenced by the individual difference of the subject greatly. Therefore, averaging the temperatures at the distal end of Case 2 and 3 with a few number of subjects, seems to be most influnced by individual differences.

Comparison of surface temperatures of socks

Figure 14 presents a comparison between values obtained from analysis and actual measurements of the surface temperature of socks in each case. The analysis value is lower than actual measurements by 1–3°C in each case.

This is regarded as attributable to the considerable dispersion of data according to individual differences. At measuring point (3) on the soles, a

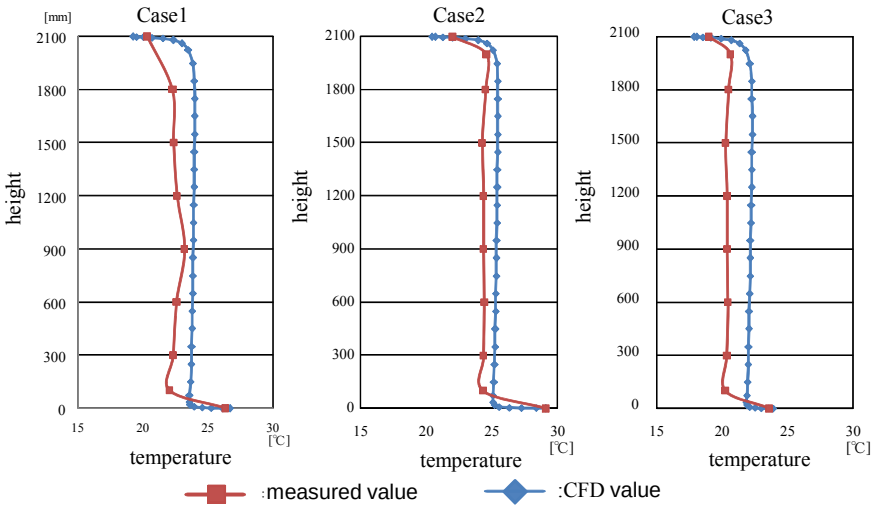

Figure 10 Distribution of vertical temperatures (Pole 1)

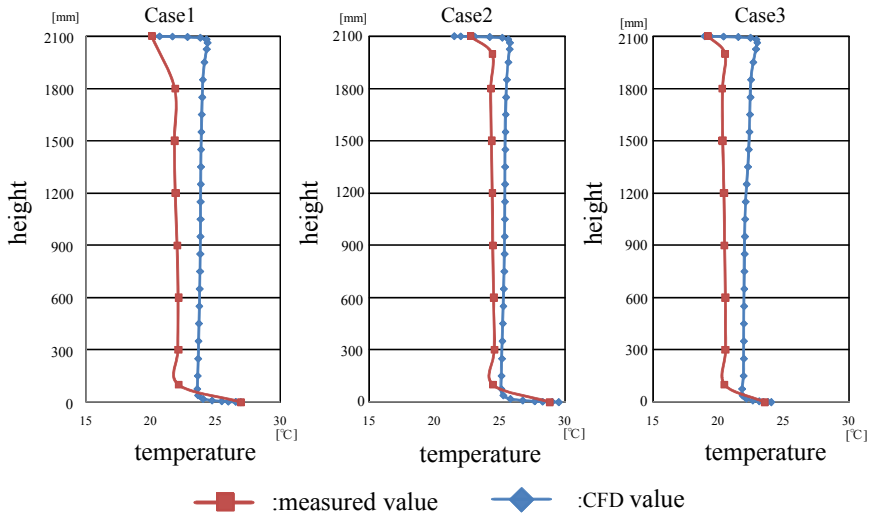

Figure 11 Distribution of vertical temperatures (Pole 2)

trend is apparent by which the analysis value of surface temperatures of socks is lower than actual measurements. This is regarded as attributable to the fact that the measuring point (3) is at the plantar arch and the contact condition of the heel and floor surface showed a difference between the values elicited from analyses and actual measurements. Furthermore, differences between values obtained from analysis and actual measurements are greater in terms of surface temperature of socks than for the skin surface temperature of soles. This is regarded as attributable to the fact that thermal resistance for analysis of socks area differs from actual measurements.

Distribution of heat current

Table 4 presents a comparison between values obtained from analysis and actual measurements of contact conduction heat flow in each case. The difference of both in each case is less than about 0.5W; their trends mutually agree. In Case 1, although it is an extremely small value, the direction of heat flow in actual measurements and analysis is reversed. This difference from actual measurement results is regarded as extremely close to the measurement accuracy limit of the heat flow meter. The number of human subjects should therefore be increased to obtain more adequate values.

Human body surface temperatures

Figure 15 shows a surface temperature distribution of the human model in each case by CFD analysis. In Case 3 of the floor surface temperature 23°C, the upper body temperature became lower than that of other cases. This is regarded as attributable to the air temperature of the ambient environment of the human body model being 2–3°C lower than that in Case 1 and 3–4°C lower than in Case 2.

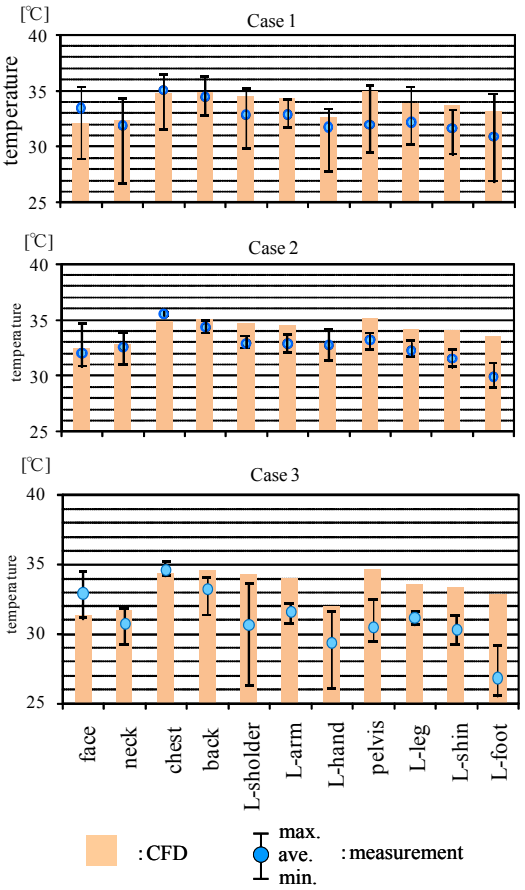

Figure 12 Comparison of clothes surface temperatures.

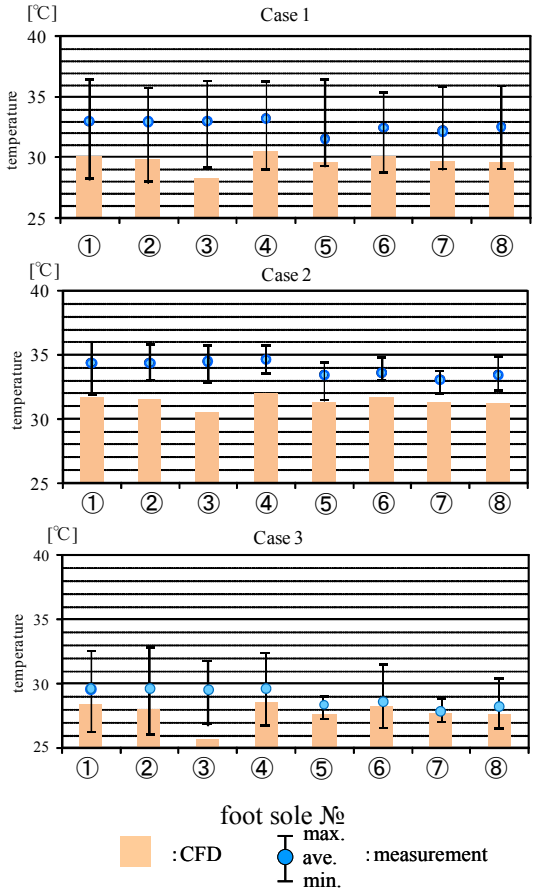

Figure 14 Comparison of socks surface temperatures.

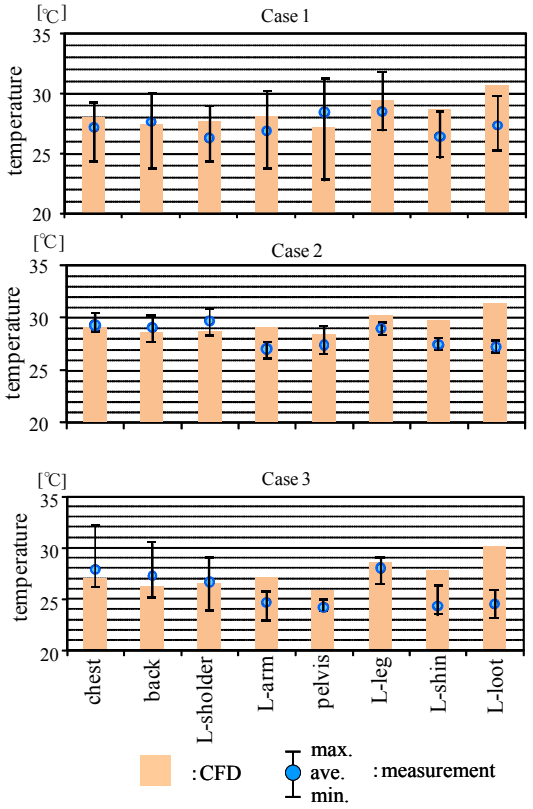

Figure 13 Comparison of skin surface temperatures.

Table 4 Comparison of heat flow at floor contact areas.

Case	measured value [W/m^2]			CFD value [W/m^2]
	minimum	maximum	average	
Case1	-1.504	1.196	-0.180	0.126
Case2	0.751	1.119	1.956	0.260
Case3	0.629	-1.490	-0.537	-0.145

Distribution of room temperature

Figure 16 shows a distribution of the wall surface temperature of each case obtained using CFD analysis. In Cases 1–3 shown by floor surface temperature, the average surface temperature excluding the heat bridge portion at the north plane and east plane is about 23°C in Case 1, 24°C in Case 2, and 21°C in Case 3. Regarding the cause for the upper body temperature of the human model in Case 3 being lower than that of either Case 1 or 2, the influence of radiative cooling from the wall surface is considered in addition to the low air temperature of the ambient environment of the human body model.

Figure 17 presents the temperature distribution at the vertical section at the center of room by CFD analysis. It is possible to confirm the upward thermal flow because of the influence of heat generation by the human body. It is possible to confirm in each case that the uniform temperature

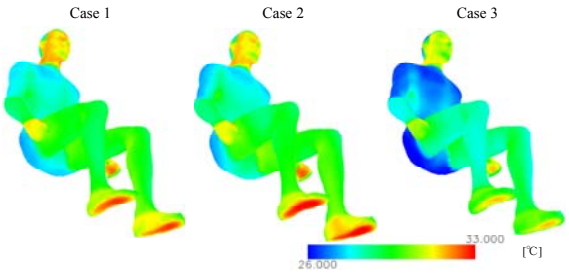

Figure 15 Surface temperature distribution of the human body model using CFD analysis

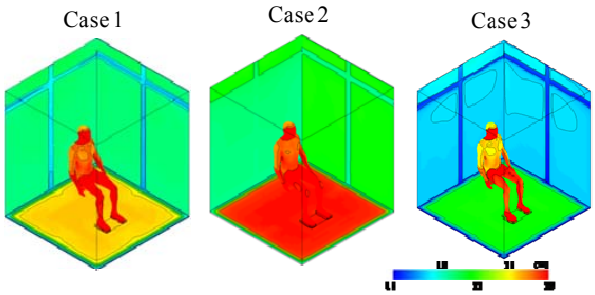

Figure 16 Wall surface temperature distribution obtained using CFD analysis.

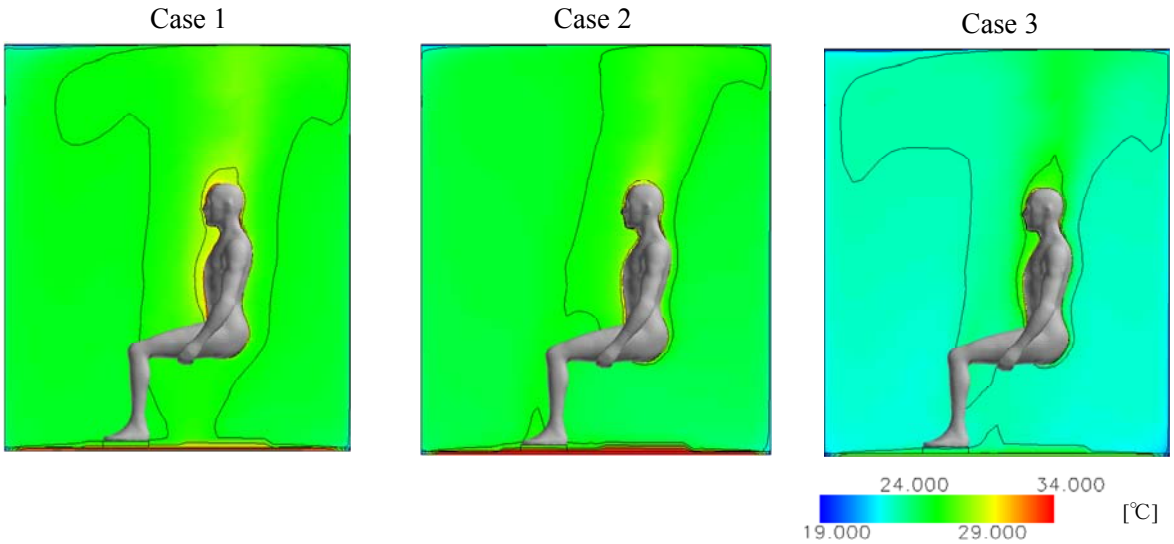

Figure 17 Temperature distribution of a vertical section obtained using CFD analysis.

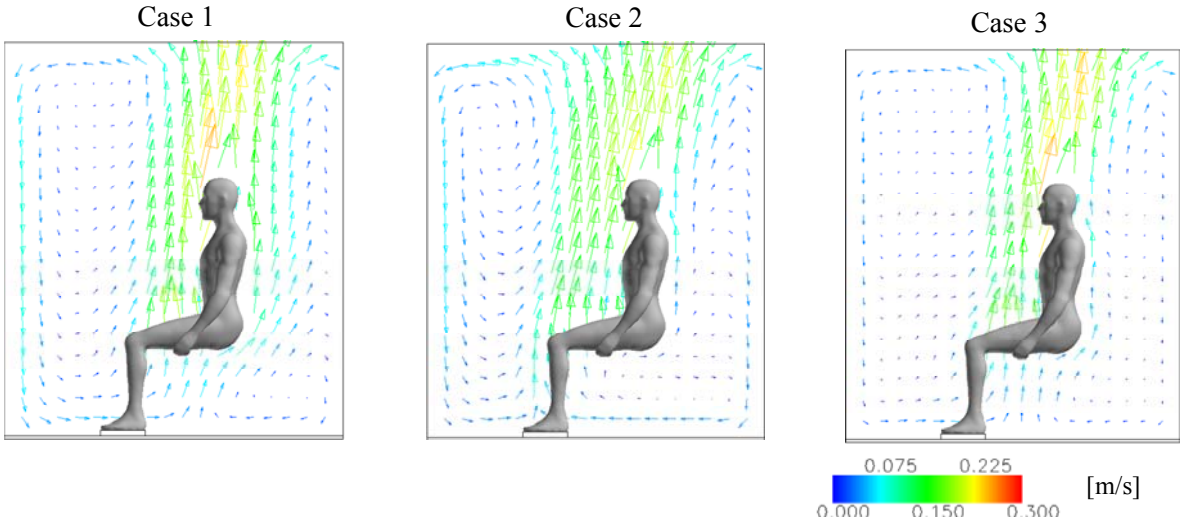

Figure 18 Air current distribution at a vertical section obtained using CFD analysis.

field, one characteristic of floor radiation heating, is formed.

Comparison of wind velocity in the room Figure 18 shows the distribution of air currents at a vertical section at the center of the room obtained using CFD analysis in each case. It is possible to confirm the upward flow of a strong air current because of heat generation by the human body in the vicinity of the

human body model. Extensive convection of air is generated in front of and behind the human body. In Case 3, air convection became small in front and behind the human body model and around the wall surface.

CONCLUSION

This report describes results of CFD analysis of a floor-heated room interior, which was performed using contact and thermal conduction with a thermal mannequin, to grasp heat transfer processes such as conduction, convection, and radiation systematically and in detail, with comparative study and actual measurement experiments performed with human subjects. Results confirmed that human body environments such as skin surface temperature, clothes surface temperature, heat flow, etc. were generally reproducible using CFD. As an initial step, comparison between actual measurements and CFD was performed targeting an empty floor of a heated room interior. Differences between actual measurements and values obtained from analysis of distribution of vertical temperature in the room were generally within 1°C; wall surface temperatures are also generally within 1°C: thereby good agreement was confirmed. Regarding the reason for differences between the air temperature and wall surface temperature, differences of the body surface area were considered. Further analyses should be made in consideration of differences of physical constitution between human subjects and the human body model used for CFD. Furthermore, the method of setting of boundary conditions of human body extremities such as limbs and thermal resistance of clothes should be reviewed considering the air layer between clothes and skin.

ACKNOWLEDGEMENTS

The authors express their thanks to Mr. Y. Kato (Kajima Corporation), Ms. H. Kanai (Tokyo Electric Power Co.), and Ms. K. Yamaguchi (Mitsui Home Co. Ltd.) for their great cooperation extended during actual measurements and analyses.

REFERENCES

Ito K., Hotta T. (2006). Development of Virtual Manikins and Its Grid Library for CFD Analysis, Transactions of the Society of Heating, Air-Conditioning and Sanitary Engineers of Japan, pp.27-32.

Kajiya R., Hiruta K., Sakai K., Kurabuchi T., Iwamoto S., Kubo R. (2009). Examination of the Reproducibility of the Phenomena about the Thermal Environment of the Heating Room by CFD, Proceeding of Room Vent 2009, pp.942-949.

Kajiya R., Sakai K., Ono H., Furuya M., Sudo S. (2010). Thermal Environment Prediction using CFD with a Numerical Thermal Mannequin in a Floor Heating Room, The 7th International Conference on Indoor Air Quality, Ventilation and Energy Conservation in Buildings, IAQVEC2010.

Ogasawara T., Kurabuchi T., Fukada K. (2009). A Study on Evaluation of Thermal Environment of a Heating Room Using Computational Thermal Mannequin, Proceeding of Room Vent 2009, pp.1377-1383.

Omori T., Tanabe S. (2007). Coupled Simulation of Convection-Radiation-Thermoregulation for Predicting Human Thermal Sensation, Proceedings of Roomvent 2007, pp.81.

Omori T., Tanabe S. (2009). Influence of Building Insulation Performance and Heating Systems on Thermal Environment and Energy Performance, Proceeding of Room Vent 2009, pp.891-897.

Tanabe S., Arens E., Zhang H., Mandsen (1994). Evaluating Thermal Environments by Using a Thermal Mannequin with Controlled Skin Surface Temperature, ASHRAE Transaction, 100-1, pp.39-48.